Available online at www.sciencedirect.com
ScienceDirect
Journal of the European Ceramic Society 29 (2009) 1755–1762
www.elsevier.com/locate/jeurceramsoc

Copper tracks processing on alumina by laser cladding: Elaboration and characterization

S. Menecier, J.C. Labbe, P. Lefort *

CNRS, UMR 6638, SPCTS, University of Limoges, 123 avenue Albert Thomas, 87060 Limoges Cedex, France

Received 19 April 2008; received in revised form 22 October 2008; accepted 23 October 2008
Available online 6 December 2008

Abstract

A laser process allows achieving in air electrical tracks on alumina substrates with an electrical conductivity of 5.10^6 S m^{-1}. Copper paste was first put on alumina substrates and it was heated following a narrow track (c.a. 400 μm wide). Copper melted and oxidized partially during treatment forming cuprite Cu_2O. A reaction occurs between Cu_2O and alumina substrates which provides, after cooling, a good bonding of the copper-based tracks onto the substrates. Conditions of laser exposure have to be sharply controlled: if insufficient, tracks do not adhere to the substrate, and if too long, alumina substrates are hollowed, cracked, with vaporizations of copper and ejections of alumina. However the feasibility of such a process is now established.

Keywords: Laser processing; Copper; Al_2O_3 (D); Interface (B); Joining (A)

1. Introduction

The design of copper tracks well bonded on alumina substrates is a research field for special applications in microelectronics industries. For this, laser processes can be tested because they are cheap and efficient[1–5] and some authors studied their feasibilities. It has been asserted[6] that no chemical reaction between copper and alumina could be achieved by laser cladding directly in air, but a post treatment by heating in air at 900–1000 °C for 6–14 h allowed the formation of cuprous aluminate, which favoured the bonding of copper tracks. Other authors showed that a bonding was possible only if copper was liquid.[7]

In a previous paper,[8] a preliminary study proved, in fact, the feasibility of a laser process in air. The relevant parameters were identified and quantified in order to obtain adherent and conductive copper tracks on alumina substrates: the most influent ones were the laser power and the scanning velocity. The best adhesion results were observed for low scanning velocities, but they required rather long treatments which favoured oxidation of copper by the oxygen from air.

So, an experimental compromise had to be found in order to achieve copper tracks both adherent to alumina substrates and not too much oxidized. This paper presents the best results obtained, with new investigations in order to better understand the bonding mechanism and the relationships between copper and alumina.

2. Experimental

2.1. Materials

α-alumina substrates were 4 mm thick cylinders, cut off from a full-densified alumina bar with a diameter of 25 mm (Saint-Gobain Ceramics, purity 99.7%). The cylinders were then polished and cleaned up in acetone in an ultrasonic cleaner. The mean roughness of the samples was $Ra = 1.20 \pm 0.04$ μm (roughnessmeter Hommel Tester T500).

Two copper powders (CERAC, France) of 99.5% purity with average grain sizes of 16 μm and 100 μm were used. The main metallic impurities were Ag, Fe, Al, Pb, Sn and Ti, each content being lower than 0.01%.

Two copper pastes were achieved by mixing the copper powders with a polyvinylic alcohol (PVA) chemical binder. Those pastes were then spread onto the alumina substrate by slipcasting in order to obtain a 100 μm thick layer after a 24 h air drying.

* Corresponding author.
E-mail address: pierre.lefort@unilim.fr (P. Lefort).

0955-2219/$ – see front matter © 2008 Elsevier Ltd. All rights reserved.
doi:10.1016/j.jeurceramsoc.2008.10.013

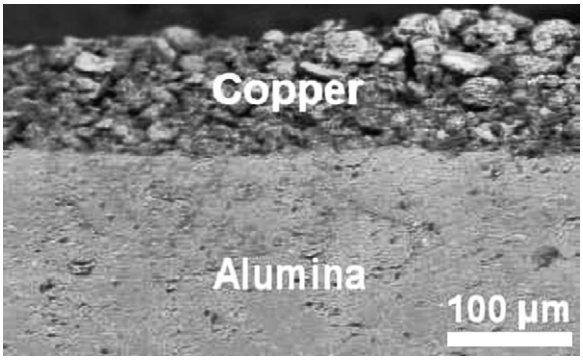

Fig. 1. Cross section of a sample before laser treatment.

The pastes had an average apparent density of c.a. 7.30 g cm^{-3}. A cross section of a so-obtained sample, before laser treatment, is presented in Fig. 1.

A 50 μm thick overlayer of a carbon paste (average grain size of 2–12 μm) could be also spread out onto the dry initial copper layer. Carbon was chosen mainly to prevent oxidation, oxygen being supposed reacting preferentially with carbon than with copper.

2.2. Process

The samples composed of alumina substrates covered by the dried copper paste were placed under a continuous infrared laser beam to create adherent copper tracks on alumina.[8] They were put on a XY table to control their position and their displacement velocity during treatment, from 0.01 to 30 mm s^{-1}. The substrates could be preheated to prevent thermal shocks thanks to a heating plate. The whole process took place in air. Fig. 2 outlines the principle of the process.

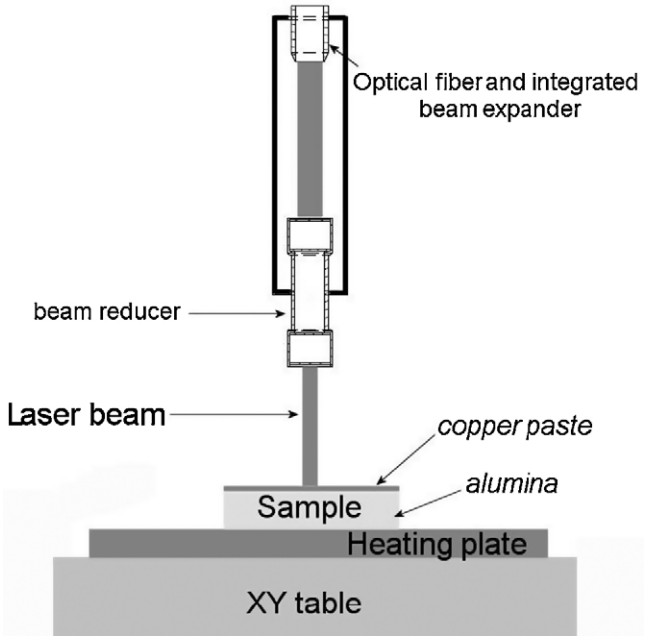

Fig. 2. Scheme of the laser process.

Table 1
Optimized parameters determined with Plackett and Burman's design of experiments.

Parameter	Value	Unit
Beam diameter	1	mm
Overlap	0	
Powder grain size	c.a. 16	μm
Preheating temperature	400	°C
Laser power	1–100	W
Scanning velocity	5.10^{-3}–100	mm s^{-1}

Concerning the laser, it was a 100 W continuous double cladded fibre one (YLR IPG Photonics, France). Its wavelength was 1072 nm with a beam profile TEM00 (Gaussian profile). The beam diameter varied from 1 to 5 mm using a lens device, and the power could be adjusted between 1 and 100 W. In these conditions, the power density received by the sample went from 50 kW m^{-2} to 130 MW m^{-2}. In the following, the power density is not given, as far as it is not a relevant parameter.[8] Indeed, it is not representative of the heat really transferred from the laser radiation to the material because this transfer is very complex and it varies, in particular, with temperature and with physical state of copper (solid powder or liquid).

In the process, six parameters could be controlled:

- The laser power;
- The laser beam diameter;
- The scanning velocity;
- The overlap between two passes of the laser beam;
- The initial grain size of the copper powder used;
- The substrate preheating.

A first technological approach[8] using a Plackett and Burman's design of experiments fixed values considered as optimal for each parameter (presented in Table 1). They allowed outlining the necessary compromise that had to be found between adhesion and electrical conductivity of the copper track. Nevertheless, in this work the laser power and the scanning velocity, which determined the power density, were modified according to the attempts. Adhesion of copper on alumina was always achieved by only one pass of the laser beam on the same zone (overlap = 0).

For the highest energy densities, ejections and vaporization of matter were observed during the laser treatment. In such conditions, a cold trap located just above the samples collected many spherical particles of alumina, sometimes covered with copper and/or copper oxides as seen in Fig. 3. Then, local temperature on the sample surface reached at least 2053 °C (melting point of alumina). Some agglomerates of copper grains, oxidized but not melted, were also ejected because of a thermal blast.

The gas above the substrates were analysed by UV–V emission spectroscopy from 200 to 800 nm using a Triax 320 monochromator (Jobin-Yvon, France) linked to a CCD camera. Spectramax software acquired the gas spectra. One of them is presented in Fig. 4, showing that the only metallic phase detected was copper. The Sodium D-lines at 588.99 and 589.59 nm and

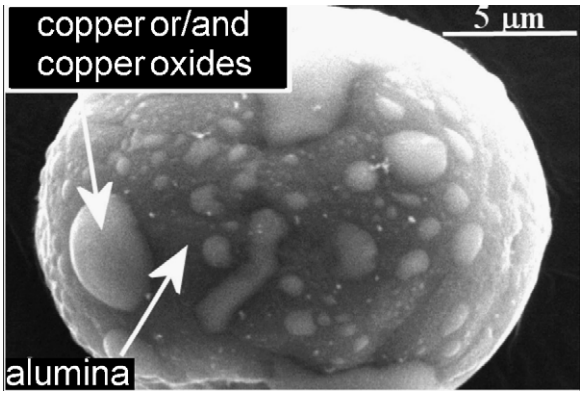

Fig. 3. Ejected alumina grain, covered with copper–copper oxides nodules.

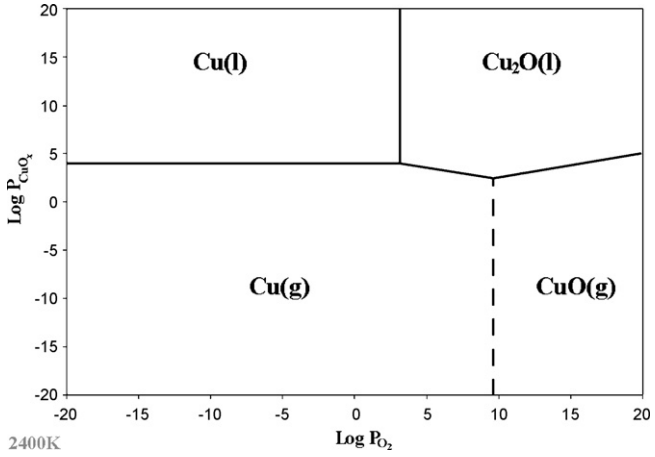

Fig. 5. Volatility diagram of copper and copper oxides at 2127 °C.

hydroxide molecular were attributed to the vaporization of the chemical binder from the copper paste. No Al element was detected, showing that alumina did not vaporize quantitatively during laser treatment. These observations were correlated with thermodynamical calculations. Fig. 5 presents the volatility diagram of copper and copper oxides at 2127 K, calculated thanks to JANAF tables.[9] It confirms that, in the process conditions (in air, i.e. with $P_{O2} \approx 0.21 \times 10^5$ Pa hence Log $P_{O2} = 4.3$), the stable phases are Cu gas, with a relatively high partial pressure (3.6×10^3 Pa), and Cu_2O liquid.

A reaction mechanism for the highest energy densities can be immediately advanced to justify those observations. It is outlined in Fig. 6. When the laser processing starts (Fig. 6a), the surface copper melts, oxidizes and vaporizes very quickly – c.a. 10 ms – (Fig. 6b); alumina also melts and it is blown away (Fig. 6c). A strong gas flow takes place, because of the temperature gradient, directed toward the middle of the track, blowing solid and liquid matter (copper, copper oxides, alumina). It is worth noting that this blowing effect was always observed, even for the lowest powers, but with weaker intensities.

2.3. Samples characterization

The phase identifications were performed with an X-ray Brüker D5000 diffractometer ($\lambda_{Cu} = 0.1541$ nm) equipped with a back monochromator. The scanned angles (2θ scale) ranged from 30 to 70° with a step of 0.015° and a 10 s exposure time. The X-ray diffractograms were indexed by using the DIFFRAC+ software (Socabim) and the JCPDS database. Morphological observations and analyses were carried out with

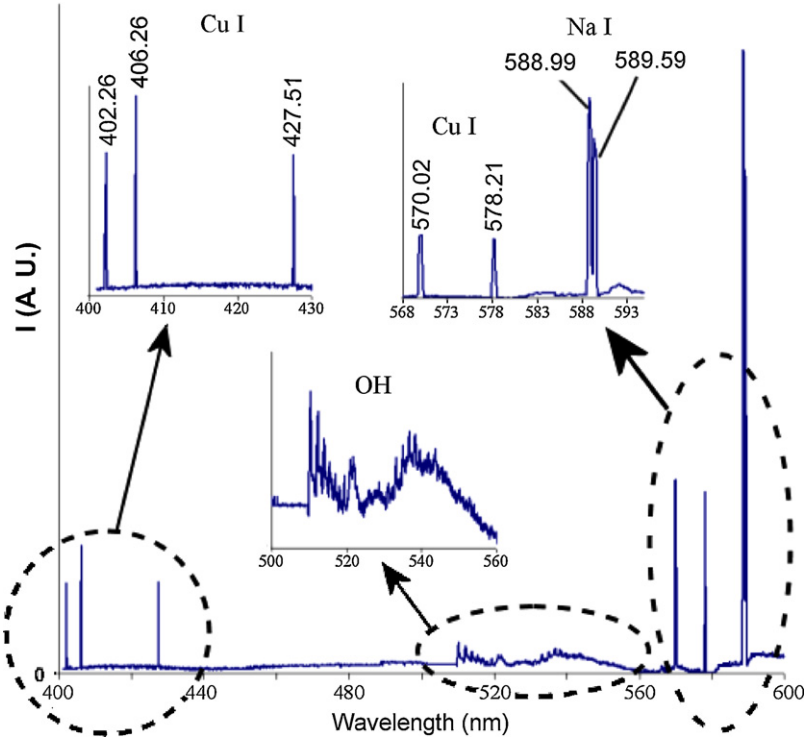

Fig. 4. Typical spectrum of gas detected above the substrate during laser treatment.

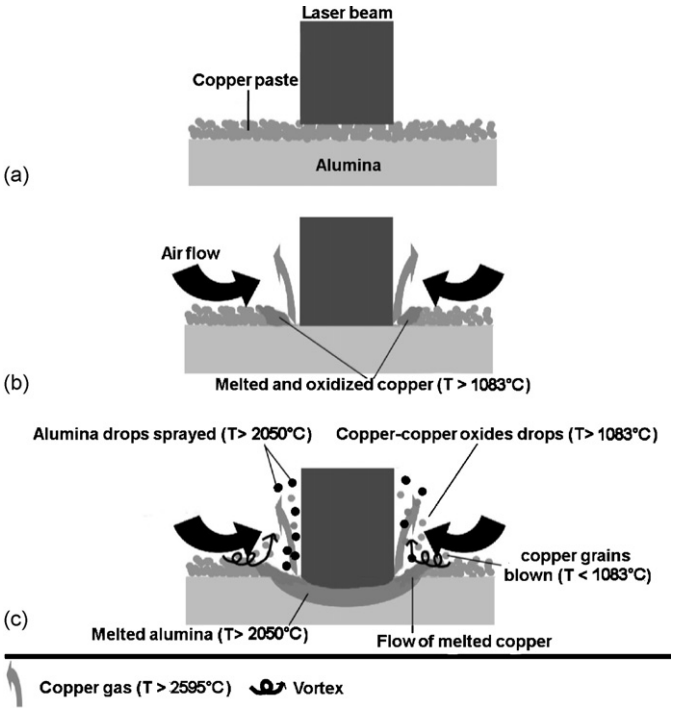

Fig. 6. Effects of the most energetic laser treatment on the samples: (a) the laser beam arrives, (b) vaporization of copper and enhancing of the gaseous flows, (c) melting of the alumina substrate and spraying of melted matter.

a Scanning Electron Microscope (Philips XL30) equipped with EDS, and with an EPMA CAMECA SX 100 (IFREMER, Brest, France).

3. Results

3.1. Samples without carbon

Several experiments have been carried out with different scanning velocities and laser powers. The resulting copper tracks always exhibited the same external morphology due to the melting of the copper paste under the laser beam.

In cross section, the tracks presented profiles like volcano, with a central crater and edges rising higher than the initial level of the copper paste. In top sight, they were linear, with a width lower than the diameter of the laser beam (attributed to the Gaussian profile of the laser beam and to the thermal conductivity of the sample), and with waves c.a. 100 μm distant from each other. Fig. 7a and b give respectively the typical schematic profile and top view of the tracks. Fig 7c presents a top view micrograph of a track obtained with a laser power of 40 W and a scanning velocity of 10 mm s^{-1}. XRD of the surface identified Cu, Cu_2O, traces of CuO, but no cuprous aluminate.

So, during the laser process, the copper grains partially oxidized, sintered and melted simultaneously. For instance, Fig. 8 presents the surface of an alumina–copper sample after laser treatment. It shows different areas: a central melted zone where the middle of the laser beam passed and a peripheral one where copper grains sintered. Temperature reached at least the melting

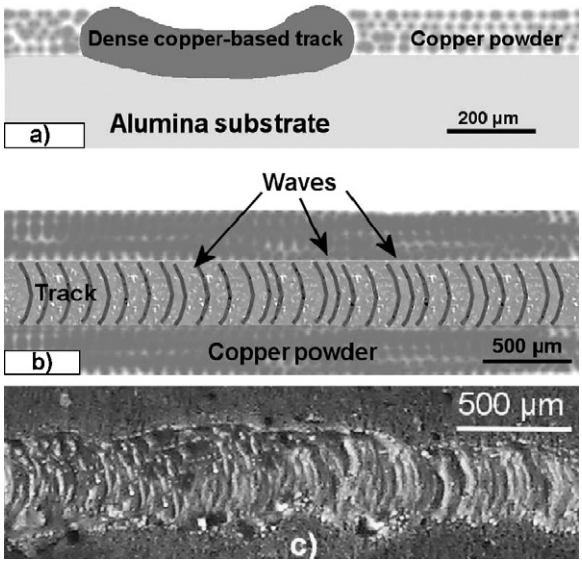

Fig. 7. Schematic representation of cross section (a) top sight obtained after laser processing (b) and micrograph of a track as observed (c).

point of copper (T_f = 1085 °C) in the melted zone whereas in the sintered zone, temperature could be evaluated between T_f and Tamann temperature (≈2/3 T_f to T_f/2).

Alumina substrates were sometimes not affected by the treatment, as illustrated in Fig. 9, in the case of a sample treated with a laser power of 60 W and a scanning velocity of 30 mm s^{-1}, giving a relatively satisfying electrical conductivity (c.a. 2.10^6 S m^{-1}) but with a poor adherence (the tracks were easily pulled off with nail).

By increasing energy densities, adhesion was improved, but Fig. 10a shows that, with the highest energy densities, the laser treatment became disastrous for alumina substrates: with a laser power of 80 W and a scanning velocity of 1 mm s^{-1}, the alumina substrate was cracked and presented (see Fig. 10b) a remarkable stack of alumina (in grey) and copper-based phases (in white)

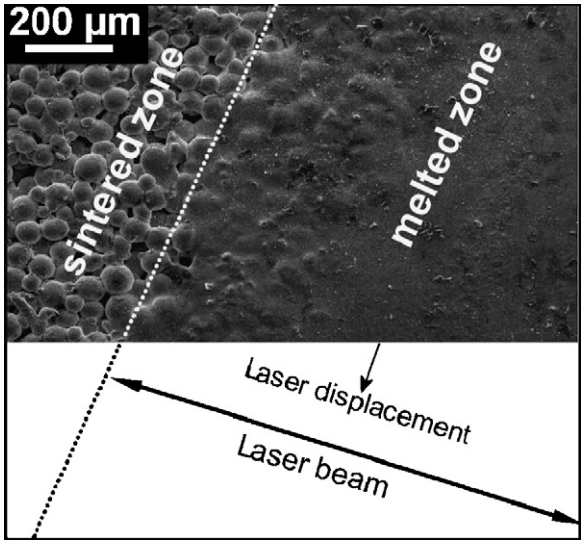

Fig. 8. Micrograph of the surface of a laser treated sample (P = 40 W, v = 20 mm s^{-1}).

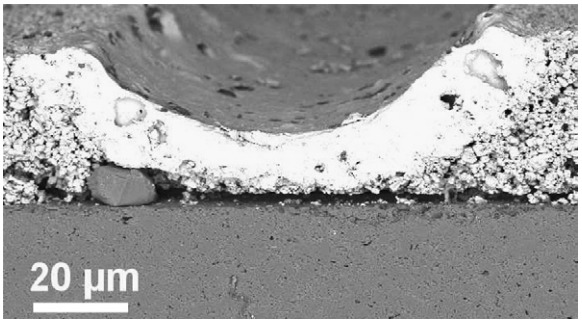

Fig. 9. Cross section of a track obtained with a laser power of 60 W and a scanning velocity of 30 mm s^{-1}.

identified by EPMA as mainly composed of cuprite Cu_2O and non-oxidized copper.

The best tracks obtained without carbon layers were achieved using a scanning velocity of 20 mm s^{-1} and a laser power of 60 W. The result is presented in Fig. 11a. In this case, the track was still convex, but alumina rose along the track (marked by arrows in Fig. 11b). This confirmed that during the process, copper, more fusible, melted first and, when alumina melted, the heavy liquid copper displaced the molten alumina and forced it to rise around it. This track had a very good adhesion to the substrate, but its electrical conductivity decreased to c.a. 6.10^4 S m^{-1} which is three orders of magnitude less than that of pure copper. By comparison with Fig. 9, the scanning velocity decreasing from 30 to 20 mm s^{-1} had two main consequences:

(i) The Heat Affected Zone (HAZ) depth increased, allowing the melting of the alumina substrate;

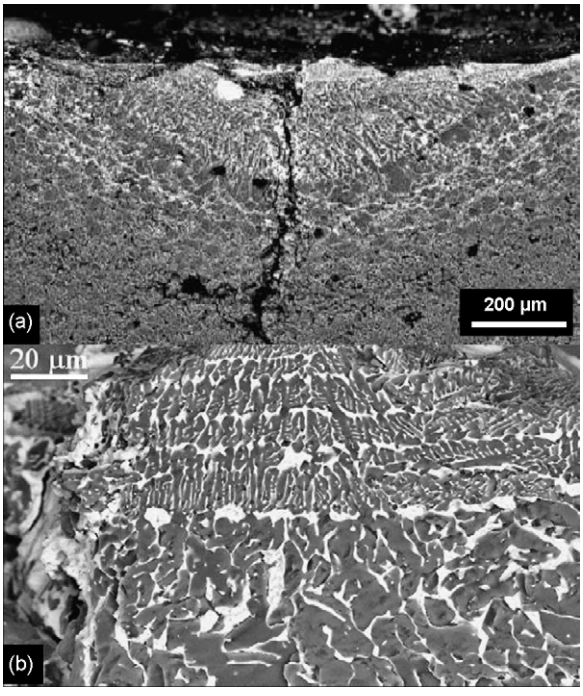

Fig. 10. Cross section of a track obtained with a laser power of 80 W and a scanning velocity of 1 mm s^{-1}, (a) overview and (b) details.

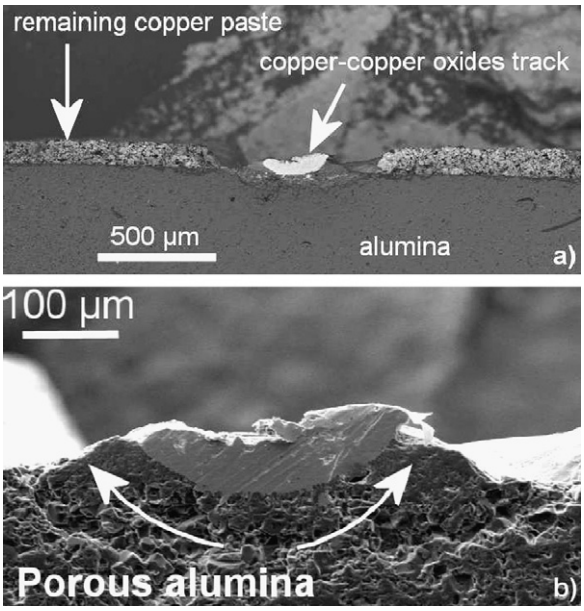

Fig. 11. Cross section of a satisfying track obtained with a laser power of 60 W and a scanning velocity of 20 mm s^{-1}: general view (a) and zone of the track (b).

(ii) The longer exposure time led to a more extended oxidation of copper, which reduced the electrical conductivity of the track.

Indeed, as far as Cu_2O and CuO are not good electrical conductors (they are semi-conductors), the presence of these oxides, probably located at the grain boundaries, has necessarily a disastrous effect on the overall electrical conductivity of the tracks. It was the reason why attempts were made using a cover layer of carbon.

3.2. Samples with a carbon layer

In this case, the samples were no longer preheated to avoid carbon oxidation before laser treatment. The most satisfying tracks were obtained with a laser power of 40 W and a very low scanning velocity (0.01 mm s^{-1}). A cross section of such a sample is presented in Fig. 12a. It shows that the track penetrated deep inside the substrate (up to c.a. 200 µm), which was not disrupted but where some microcracks appeared near the track. The electrical conductivity of the track was about 5.10^6 S m^{-1}, which indicates that copper oxidation was rather limited. A direct comparison with samples not covered by a carbon layer is difficult, because the same laser treatment (40 W, 0.01 mm s^{-1}) led to samples broken, with morphologies near the fracture zone like that of Fig. 10 and with very high resistivities.

Now, the samples treated with such a multicoating technique were the best obtained with the present laser process. EPMA maps of Fig. 12 present the distribution of elements aluminium (Fig. 12b), oxygen (Fig. 12c) and copper (Fig. 12d). The mapping of carbon is not possible because the sample was covered with carbon for analyses. They show that the alumina substrate has been hollowed and that alumina and copper-based phases were mixed together.

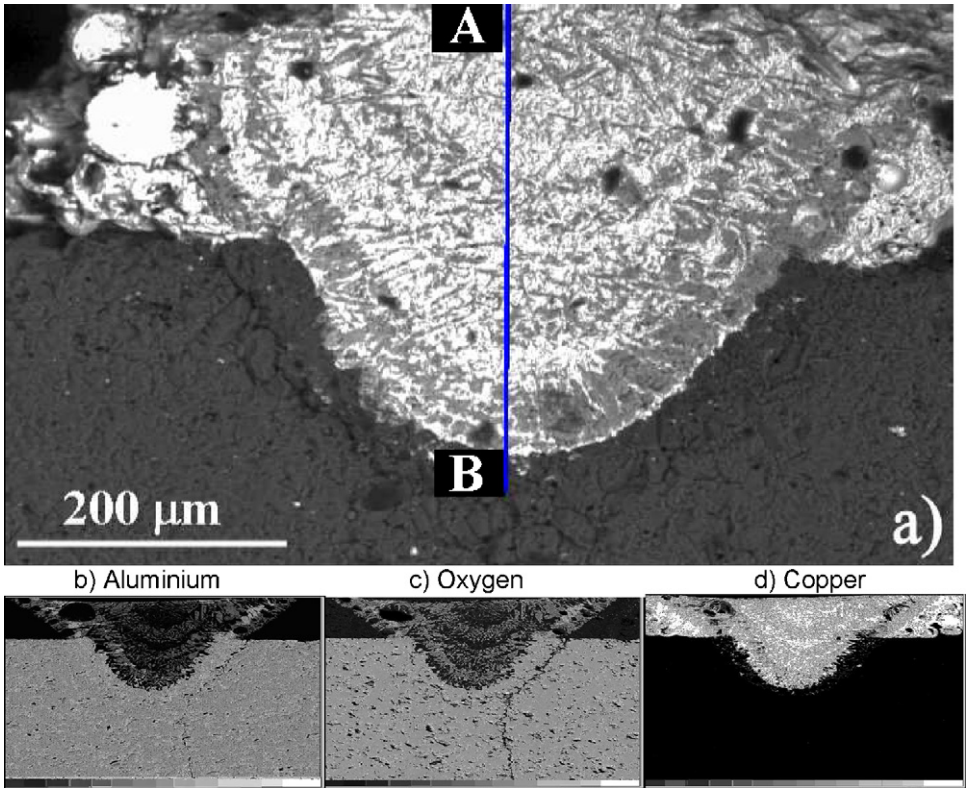

Fig. 12. Cross section of a track achieved with a carbon overlayer (a) and EPMA mappings of aluminium (b), oxygen (c) and copper (d).

A concentration profile of the elements Al, Cu and O following the AB line drawn in Fig. 12a is given in Fig. 13. It confirms the inhomogeneity of the solidified track. Parts such as those marked (1) were composed of copper and oxygen, with a large majority of element copper, corresponding to a composition of c.a. 50% of metallic copper and 50% of cuprite Cu_2O (proportions variable according to the considered zone), while parts like (2) contained copper, aluminium and oxygen in relative atomic respective content of 25, 25 and 50% that are those of the phase $CuAlO_2$ (delafossite). The presence of this phase can be explained by a reaction such as

$$Cu_2O + Al_2O_3 = 2CuAlO_2 \quad (1)$$

following a previous oxidation of copper into Cu_2O. This cuprite phase, which certainly appeared at the interface copper/air, was liquid under the laser beam, such as the metallic copper. Then, the so-formed cuprite could reach alumina because of thermal convection flows inside the liquid phase and react with it according to Eq. (1). In addition to the justification of reaction (1), such a liquid convection, sometimes called Marangoni convection, certainly causes motions at the surface of the liquid phase that may also explains the "waves" observed at the surface of the copper tracks after solidification (see Fig. 7c).

4. Discussion

The copper-based phases which can exist at temperatures going between the copper and the alumina melting points (1085–2053 °C) are given by thermodynamical calculations

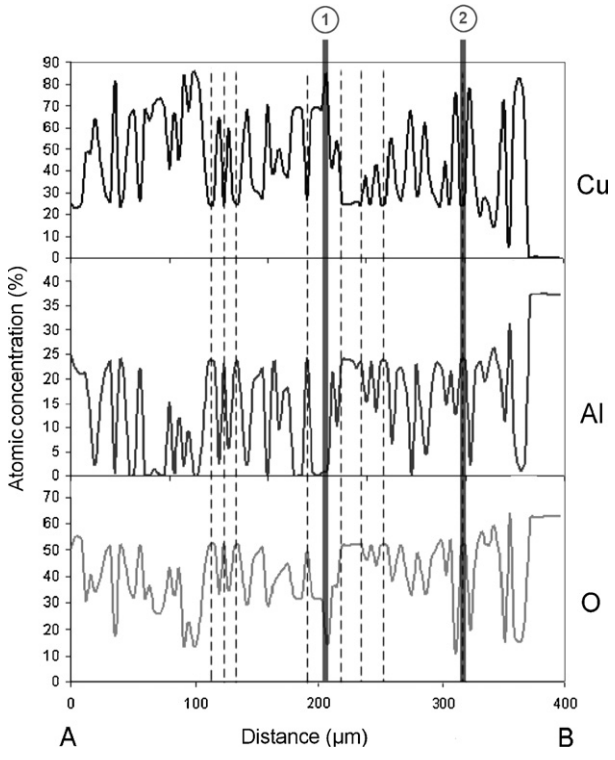

Fig. 13. Elements concentrations from A to B (see Fig. 12a) determined by EPMA.

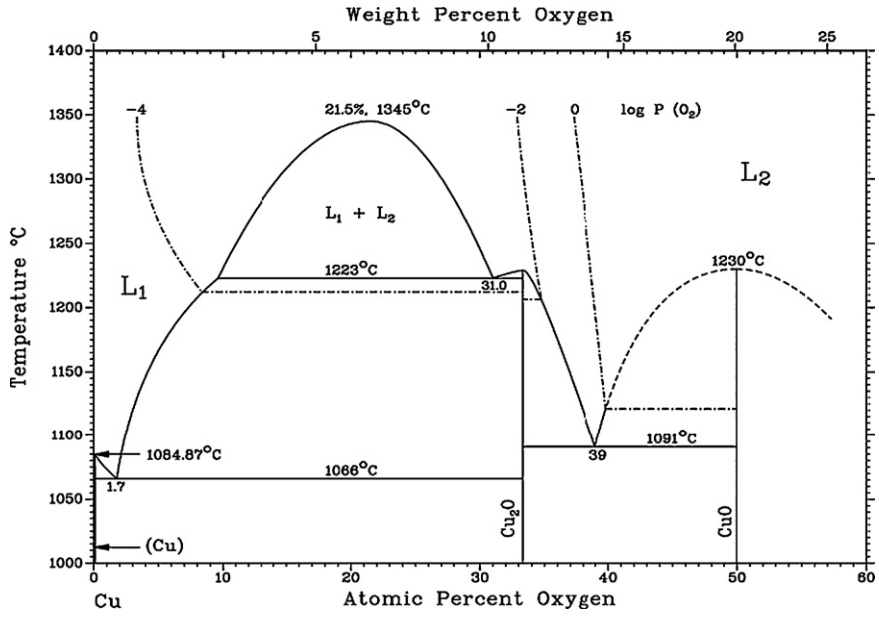

Fig. 14. Cu–O phase diagram.

such as those summarized in Fig. 5. At these temperatures, in the air, the stable copper oxide is Cu_2O, which is solid below 1235 °C and liquid above this temperature, while the gaseous phase is always composed of metallic Cu. The intense gaseous convection current, mentioned above and schematized in Fig. 6, certainly provided an important flow of fresh oxygen at the sample surface, so that oxidation of copper following

$$4Cu_{(l)} + O_{2(g)} = 2Cu_2O_{(l)} \quad (2)$$

rapidly occurred. At temperatures higher than 1345 °C the two liquids phases Cu and Cu_2O are entirely miscible and form only one liquid, as it can be seen in Fig. 14, which presents the phase diagram of copper and its oxides.[10] Hence, under the laser beam, the liquid phase certainly contained a mixture of metallic atoms of copper and ions Cu^{2+} and O^{2-}. It was probably very reactive when it was in contact with the ionic oxide Al_2O_3 which was just below it, and it could easily dissolve it, at least partially, following an overall reaction which can be written

$$[Cu, xCu^{2+}, x/2O^{2-}]_{(l)} + yAl_2O_{3(s)} = [Cu, xCu^{2+}, 7x/2O^{2-}, 2yAl^{3+}]_{(l)} \quad (3)$$

where x and y are coefficients representing the content of cuprite and alumina dissolved in the liquid phase.

The quantity of fused copper can be estimated by considering the initial copper paste volume: for a track's length of 1.0 μm, the volume of copper is c.a. 45×10^3 μm^3 (taking in account the initial thickness of copper of 100 μm, and a compacity of the green layer of copper of c.a. 0.65). Concerning alumina, the quantity dissolved can be evaluated, for instance in Fig. 12a, on the basis of the semi-circular profile of the hollowed area: for a length of 1.0 μm, the volume of alumina dissolved is equal to 34×10^3 μm^3. Globally, this would lead to a liquid phase containing 20 at% of Al, 49 at% Cu and 31 at% O. A comparison with the contents determined by the microanalysis of Fig. 13 shows that these data are compatible, since the average content measured by EPMA is c.a. 15 at% of Al, 50 at% Cu and 35 at% O, this last content being rather higher because of the copper oxidation by air (Eq. (1)).

Now, the so-determined composition allows putting this phase in a ternary phase diagram Cu/Al/O such as that of Fig. 15, given at 1000 °C[11]: the original liquid phase composition can be represented by the cross located in the triangle $Cu/CuAlO_2/Cu_2O$. It can be seen on this representation that, during cooling, a demixing is possible, that would give the three phases Cu, Cu_2O and $CuAlO_2$ in respective contents 56, 11 and 33 mol%, i.e. 28, 19 and 53 vol%., and it was precisely the phases identified by microanalysis (see Section 3.2 and Figs. 12 and 13).

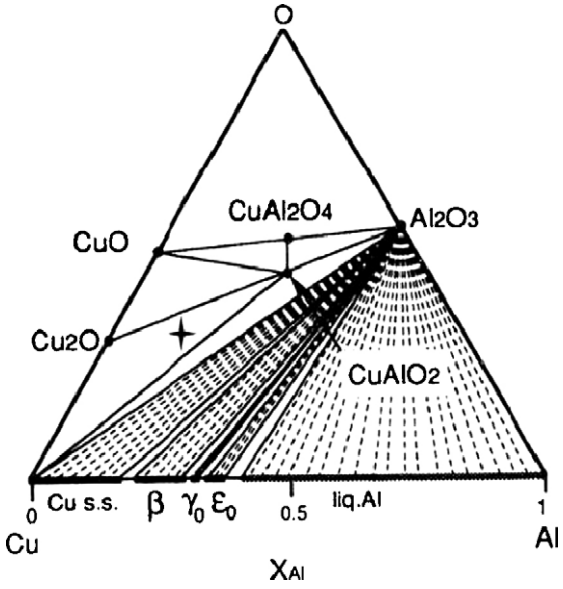

Fig. 15. Ternary diagram, Cu/Al/O at 970 °C.[10] Cross shows the composition of the melted bath, determined experimentally.

Moreover, phases demixing generally give ordered phases, so that it could explain very well the phases observed as well in Fig. 10 as in Fig. 12, where alumina and cuprous phases appears as ordered, in a stacking not compatible with the random mixing which would result from the only thermal flow, especially by considering the great difference of densities between the different phases.

Lastly, this mechanism proposal provides also a good explanation for the erosion of the alumina substrates, generally observed (see Figs. 10 and 12a and schematic representation of Fig. 6). As far as the high temperature zone is very narrow on the surface of the samples, one may suppose that, when the laser exposition stops, the liquid phase demixes, solidifies and cools very quickly: then, the composition of the final copper phase obtained depends on the quantities of oxygen fixed through reaction (2) and on that of alumina dissolved via Eq. (3).

5. Conclusion

This study presented promising results concerning the design of electrical copper tracks on alumina substrates by using a simple laser process. The most important difficulty is to control copper oxidation, which plays an ambivalent role: on one hand, even in the case where metallic copper is the major phase, the presence of oxygen and aluminium inside it has for consequence a drastic decreasing of the electrical conductivity of the track; but, on the other hand, oxygen inside the copper-based phases insures simultaneously, via the cuprous aluminate formation, a kind of physicochemical continuity at the alumina/track interface which is well known to favour the bonding between metals and ceramics.[12,13] Otherwise, as the use of an inert gas would complicate the process, the multilayer technique, presents several advantages: carbon overlayer greatly improved the quality of tracks copper obtained by limiting oxidation of copper, but without preventing delafossite to form, this phase favouring chemical bonding between copper and alumina. Nevertheless, this process needs again to be improved in particular in order to control the convection flow of the liquid phases, in the molten bath, a possibility being perhaps a fine tuning of the laser power and the scanning velocity.

References

1. Oberländer, B. C. and Lugscheider, E., Comparison of properties of coatings produced by laser cladding and conventional methods. *Mater. Sci. Technol.*, 1992, **319**(8), 657.
2. Webber, T., Advances in the applications of laser cladding of multi-dimensional part geometries. In: Proceedings of SPIE, The International Society for Optical Engineering, Bellingham, Washington, 744, 1987, 137.
3. Atamert, S. and Bhadeshia, H. K. D. H., Comparison of the microstructures and abrasive wear properties of stellite hardfacing alloys deposited by arc welding and laser cladding. *Metall. Trans. A*, 1989, **20**, 1037.
4. Baldus, O., Schreck, S. and Rohde, M., Writing conducting lines into alumina ceramics by a laser dispersing process. *J. Eur. Ceram. Soc.*, 2004, **24**, 3759.
5. Schneider, M., Laser cladding with powder. Ph.D. thesis. Enschede, Netherlands: Twente University; 1998.
6. Shepeleva, L., Medres, B., Kaplan, W. D. *et al.*, Laser induced Cu/alumina bonding: microstructure and bond mechanism. *Surf. Coat. Tech.*, 2000, **125**, 40.
7. Curicuta, V., Alexander, D. R., Liu, Y., Robertson, B. W. and Poulain, D. E., Furnace and laser methods of bondings metals to ceramics: interface investigation. *Mater. Sci. Eng. B*, 2000, **68**, 196.
8. Menecier, S., Jarrige, J., Labbe, J. C. and Lefort, P., Identification of parameters involved in the bonding of copper tracks on alumina substrates by a laser process. *J. Eur. Ceram. Soc.*, 2007, **27**, 851.
9. Chase, M. W., Curnutt, J., Downey, J. *et al.*, JANAF thermodynamical Tables, 1982 Supplement. *J. Phys. Chem. Ref. Data*, 1982, **11**(3).
10. Massalski, T., *Binary Alloy Phase Diagrams*. American Society for Metals, Metals Park, OH, 1990, p. 1447.
11. Rogers, K. A., Trumble, K. P., Dalgleish, B. J. and Reimanis, I. E., Role of oxygen in microstructure development at solid-state diffusion bonded Cu/Al2O3 interfaces. *J. Am. Ceram. Soc.*, 1994, **77**, 2036.
12. Valette, S., Trolliard, G., Denoirjean, A. and Lefort, P., Iron/wüstite/magnetite/alumina relationships in plasma coated steel: a TEM study. *Solid State Ion.*, 2007, **178**(5–6), 429.
13. Zanchetta, A., Lortholary, P. and Lefort, P., Ceramic to metal sealings: interfacial reactions mechanism in a porcelain-kovar junction. *J. Alloys Compounds*, 1995, **228**, 86.